

Heat transfer enhancement in a turbulent natural convection boundary layer along a vertical flat plate

Toshihiro Tsuji *, Tsuyoshi Kajitani, Tatsuhiko Nishino

Department of Environmental Technology, Graduate School of Engineering, Nagoya Institute of Technology, Gokiso-cho, Showa-ku, Nagoya 466-8555, Japan

Received 17 March 2007; accepted 28 April 2007

Available online 27 June 2007

Abstract

An experimental study on heat transfer enhancement for a turbulent natural convection boundary layer in air along a vertical flat plate has been performed by inserting a long flat plate in the spanwise direction (simple heat transfer promoter) and short flat plates aligned in the spanwise direction (split heat transfer promoter) with clearances into the near-wall region of the boundary layer. For a simple heat transfer promoter, the heat transfer coefficients increase by a peak value of approximately 37% in the downstream region of the promoter compared with those in the usual turbulent natural convection boundary layer. It is found from flow visualization and simultaneous measurements of the flow and thermal fields with hot- and cold-wires that such increase of heat transfer coefficients is mainly caused by the deflection of flows toward the outer region of the boundary layer and the invasion of low-temperature fluids from the outer region to the near-wall region with large-scale vortex motions riding out the promoter. However, heat transfer coefficients for a split heat transfer promoter exhibit an increase in peak value of approximately 60% in the downstream region of the promoter. Flow visualization and PIV measurements show that such remarkable heat transfer enhancement is attributed to longitudinal vortices generated by flows passing through the clearances of the promoter in addition to large-scale vortex motions riding out the promoter. Consequently, it is concluded that heat transfer enhancement of the turbulent natural convection boundary layer can be substantially achieved in a wide area of the turbulent natural convection boundary layer by employing multiple column split heat transfer promoters. It may be expected that the heat transfer enhancement in excess of approximately 40% can be accomplished by inserting such promoters.

© 2007 Elsevier Inc. All rights reserved.

Keywords: Natural convection; Heat transfer enhancement; Turbulent flow; Boundary layer; Flow control; Particle image velocimetry

1. Introduction

Heat transfer enhancement is a very useful technique for improvement of heat and fluid machinery performance and energy conservation. For forced convection, many heat transfer enhancement techniques have been developed and made practicable (Savill and Mumford, 1988; Han et al., 1989; Lau et al., 1991; Hu and Shen, 1996; Meinders et al., 1998; Sturgis and Mudawar, 1999). However, for natural convection, the heat transfer enhancement has been often conducted according to information on forced convection. For this reason, heat transfer enhancement tech-

niques which take account of the characteristics of natural convection in which the analogy between flow and heat transfer does not hold (Tsuji and Nagano, 1988a), are less well understood. If a heat transfer enhancement method most suitable for natural convection exists, such a technique should be positively used. For instance, spent fuels in nuclear electric power generation are stocked and cooled in containers for a long period up to recycling. Storage containers are a few meters tall in size and may be cooled by turbulent natural convection to strike a balance between economical efficiency and security. Therefore, if heat transfer enhancement for natural convection is possible, the security of fuel storage would be further increased.

Generally, fins installed on heated plates have been employed to enhance the heat transfer rate in natural

* Corresponding author. Tel./fax: +81 52 735 5333.

E-mail address: tsuji.toshihiro@nitech.ac.jp (T. Tsuji).

Notation

C	minimum distance from wall to heat transfer promoters	V, v	mean and fluctuating transverse (perpendicular to flat plate) velocities
g	gravitational acceleration	x, y, z	vertical, transverse (perpendicular to wall) and spanwise directions
Gr_x	local Grashof number $= g\beta\Delta T_w x^3/\nu^2$		
H	width of heat transfer promoters		
h	local heat transfer coefficient	<i>Greeks</i>	
I	interval of heat transfer promoters in streamwise direction	β	coefficient of volume expansion
L	height of heated plate	δ_u	integral thickness of velocity boundary layer $= \int_0^\infty U/U_{\max} dy$
l	height of starting to increase in local heat transfer coefficient with heat transfer promoters	ζ	dimensionless transverse coordinate $= (y/x)Nu_{x0}$
N	column number of heat transfer promoters in streamwise direction	Θ	dimensionless temperature $= (T - T_\infty)/\Delta T_w$
Nu_x	local Nusselt number $= hx/\lambda$	λ	thermal conductivity
N_z	number of short flat plates consisting of split heat transfer promoter	ν	kinematic viscosity
P	clearance between short flat plates consisting of split heat transfer promoter	ϕ	inclination angle of heat transfer promoters to heated plate
Pr	Prandtl number	<i>Superscripts and subscripts</i>	
T, t	mean and fluctuating fluid temperatures	–	time averaged quantities
ΔT_w	temperature difference $= T_w - T_\infty$	$()_m$	ensemble averaged quantities
U, u	mean and fluctuating streamwise velocities	0	condition without heat transfer promoter
U^*	buoyant velocity $= \sqrt{g\beta\Delta T_w x}$	max	maximum value
		w	wall condition
		∞	ambient condition

convection. However, for a turbulent natural convection boundary layer along a vertical flat plate, effective heat transfer enhancement cannot be achieved unless the fin heights exceed the boundary layer thickness (Komori et al., 1999; Misumi and Kitamura, 1999). It has been shown for this boundary layer that the maximum velocity location exists very near the wall, and a peculiar turbulent behavior arises from the mutual interference between fluid motions in the region from the wall to the maximum velocity location (inner layer) and from the maximum velocity location to the edge of the boundary layer (outer layer) (Tsuji and Nagano, 1988a,b; Tsuji et al., 1992; Hattori et al., 2001). Hence, it is expected that heat transfer characteristics of the turbulent natural convection boundary layer drastically change by inserting a drift plate into the boundary layer and controlling fluid motions in the outer layer.

In the present study, to bear out the feasibility of effective heat transfer enhancement for the turbulent natural convection boundary layer in air along a vertical heated plate, the change in heat transfer characteristics has been systematically investigated by inserting a long flat plate (simple heat transfer promoter) and short flat plates aligned at fixed intervals (split heat transfer promoter) in the spanwise direction of the boundary layer. The changes in the velocity and thermal fields of the boundary layer with these promoters have been also explored by conducting flow visualization, simultaneous measurements with hot- and cold-wires and PIV measurements.

2. Experimental apparatus and procedure

Fig. 1 shows a schematic drawing of the experimental apparatus, a long flat plate (simple heat transfer promoter) and short flat plates aligned at fixed intervals (split heat transfer promoter) and set horizontally in the spanwise direction of a vertical heated plate. The heated surface consisted of a 4 m high, 1 m wide and 2 mm thick copper plate maintained at a uniform temperature ($T_w = 60^\circ\text{C}$) by electric heaters secured on the back of the plate (Tsuji and Nagano, 1988a). The simple heat transfer promoter was a rectangular acrylic plate of 950 mm length in the spanwise direction and 1.5 mm thickness. Both ends in the spanwise direction of the simple heat transfer promoter was supported by aluminum pipes from the outside of the boundary layer as shown Fig. 1. The heat transfer characteristics were examined by changing the minimum distance C from the wall to the simple heat transfer promoter, the inclination angle ϕ of the promoter from the vertical direction and the width H of the promoter. For the split heat transfer promoter, the heat transfer characteristics were examined by varying the number N_z of short plates in the spanwise direction (both the length of each short plate and the interval between plates equal to P) under the fixed conditions of C , ϕ and H . The wall heat flux necessary to estimate heat transfer coefficients was obtained from deducing heat loss by radiation and conduction from electric power consumption of 13 heaters divided in the vertical direction

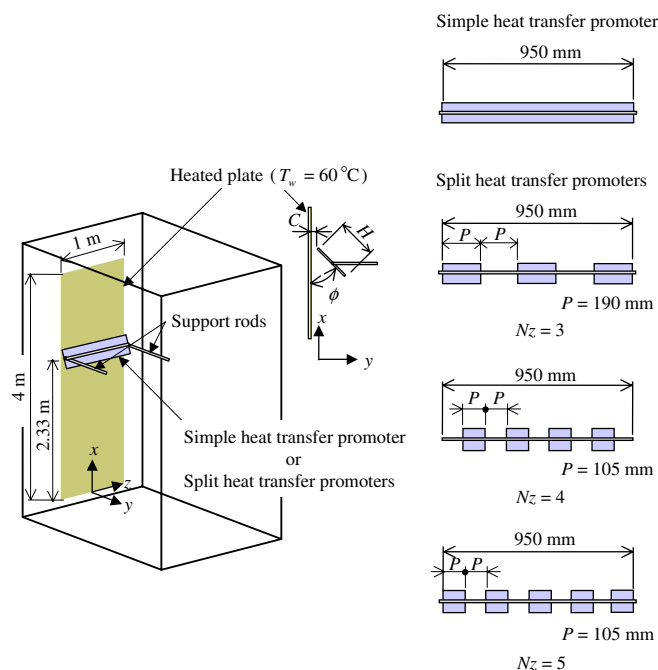


Fig. 1. Experimental apparatus, simple heat transfer promoter and split heat transfer promoters.

for heating the plate. For the boundary layer without heat transfer promoters, the heat transfer coefficients assessed in such a manner agreed well with those assessed from the fluid temperature gradient measured with a thermocouple near the wall. Although heat loss by radiation from the heated surface increased by installing heat transfer promoters, it was estimated at approximately 4% of the local wall heat flux even under the condition that the heat transfer promoters were set near the wall parallel to the heated plate. Thus, the effect of radiation was considered to be marginal.

Also, to clarify the factors affecting heat transfer and flow characteristics, the flow and thermal fields were examined by simultaneous measurements with normal hot- and cold-wires of 3.1 μm diameter tungsten (Tsuji and Nagano, 1988a) and flow visualizations including a particle image velocimetry (PIV). The heated plate used in this study is the same as that described in previously reports (Tsuji and Nagano, 1988a; Tsuji and Nagano, 1989), and the temperature condition and the measurement method are also the same. Consequently, the uncertainties of measured values with hot- and cold-wires are considered to be equal to those indicated in previously reports. For flow visualizations and PIV measurements, tracer particles (smoke) were added to the boundary layer and two-dimensional velocity fields in the x – y plane (at the center of the heated plate) were visualized by laser light sheets formed with a double pulse YAG laser. The time interval between two-pulsed illuminations was set at 2.6–4 ms so that the maximum displacement of successive particle images became approximately 10 pixels on the image plane, and the particle motions were captured by a CCD camera located approx-

imately 0.8 m apart from the object plane. The physical size of measuring areas was $150 \times 150 \text{ mm}^2$ or $200 \times 200 \text{ mm}^2$, and velocity vectors were obtained with a pattern cross-correlation method. To improve measurement accuracy, a sub-pixel algorithm was used with the assumption of a Gaussian profile for the spatial correlation. For the PIV measurements, it was confirmed that the measured results for the usual turbulent natural convection boundary layer without promoter approximately coincided with those obtained by using hot- and cold-wires.

In the experiment, the ambient temperature T_∞ was approximately 16 °C and physical properties were evaluated at the film temperature $T_f = (T_w + T_\infty)/2$, except for the coefficient of volume expansion $\beta = 1/T_\infty$.

3. Results and discussion

For two types of promoters, we discuss the streamwise variations of heat transfer coefficient and relevant data for the velocity and thermal fields obtained from flow visualization, simultaneous measurements with hot- and cold-wires and PIV measurements.

3.1. Simple heat transfer promoter

3.1.1. Heat transfer coefficients for simple heat transfer promoter

Turbulent statistics of a natural convection boundary layer along a vertical flat plate have been well investigated at the vertical location $x = 2.55 \text{ m}$ (Tsuji and Nagano, 1988b; Tsuji et al., 1992.). Therefore, the simple heat transfer promoter was placed at $x = 2.33 \text{ m}$ to examine the change in heat transfer rates near the location $x = 2.55 \text{ m}$. In the case where the center position of a simple heat transfer promoter inserted into the turbulent boundary layer is located at the distance $x = 2.33 \text{ m}$ ($x/L = 0.58$) from the leading edge of the heated plate and the configuration and size of the promoter are set as $(C, \phi, H) = (5 \text{ mm}, 45^\circ, 100 \text{ mm})$, the distribution of local heat transfer coefficients h normalized by the local heat transfer coefficients h_0 in the x direction without the promoter became as shown in Fig. 2. The region of $x/L > 0.33$ is the turbulent boundary layer. The normalized local heat transfer coefficient reaches a peak in the downstream region of the promoter and increases by approximately 37% compared with that without a promoter. Thus, it is recognized that heat transfer enhancement for the turbulent natural convection boundary layer along a vertical heated plate can be attained by inserting a simple heat transfer promoter.

Next, we examined how the peak value h_{max} of the heat transfer coefficient normalized with h_0 varied by fixing the simple heat transfer promoter at the location $x = 2.33 \text{ m}$ and changing the values of C , ϕ and H . As seen in Fig. 3, it was confirmed that the installation requirements of the promoter were consequently appropriate for $(C, \phi, H) = (5 \text{ mm}, 45^\circ, 100 \text{ mm})$. Although the effect of the

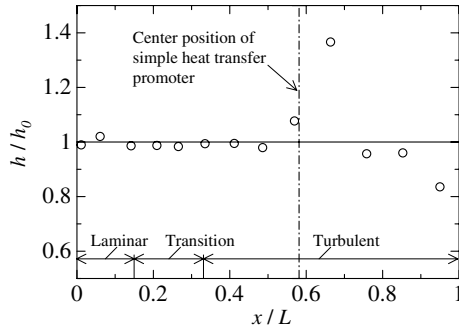


Fig. 2. Distributions of local heat transfer coefficients [simple heat transfer promotor (C, ϕ, H) = (5 mm, 45°, 100 mm)].

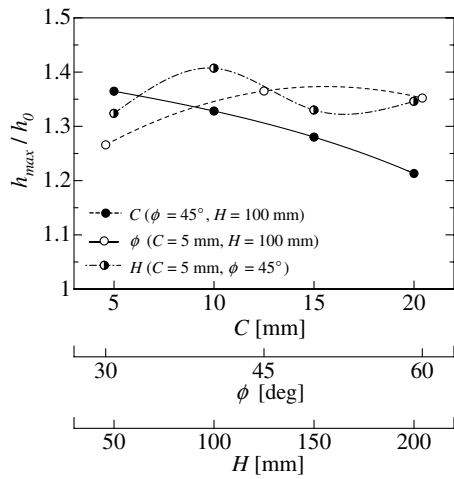


Fig. 3. Variation of maximum heat transfer coefficients with various values of C, ϕ and H for simple heat transfer promotor.

inclination angle ϕ was investigated beyond the range of that shown in Fig. 3, notable increases of the heat transfer coefficient could not be detected.

3.1.2. Flow visualization near simple heat transfer promotor

The flow behavior in the downstream region of a simple heat transfer promotor located at $x = 2.33$ m for $(C, \phi, H) = (5 \text{ mm}, 45^\circ, 100 \text{ mm})$ was visualized with smoke and laser light sheets to clarify the cause of the increase in local heat transfer coefficients. Fig. 4 shows a captured instantaneous image, and it is observed that boundary layer flows slant outside of the promotor and low-temperature fluids in the outer layer invade very near the wall with large-scale vortex motions riding out the promotor and returning to the inner layer. However, high-temperature fluids slipping through the clearances between the wall and promotor get away from the wall and impinge on large-scale vortex motions of low-temperature fluids. Consequently, it became evident that such fluid motions cause a peak value of the local heat transfer coefficient at the location ($x = 2.5\text{--}2.6$ m) where low-temperature fluids coming from the outer layer approach nearest the wall.

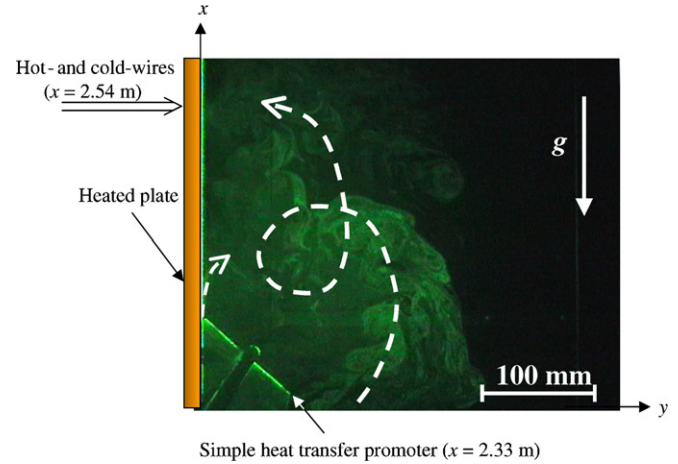


Fig. 4. Visualized fluid motions in the downstream region of a simple heat transfer promotor.

3.1.3. Hot- and cold-wire measurements of flow and thermal fields for simple heat transfer promotor

Simultaneous measurements for the thermal and flow fields with normal hot- and cold-wires were also conducted in the downstream region (the measuring position of $x = 2.54$ m indicated by an arrow in Fig. 4) of the simple heat transfer promotor located at $x = 2.33$ m for $(C, \phi, H) = (5 \text{ mm}, 45^\circ, 100 \text{ mm})$. Turbulent statistics measured for $Gr_x = 7.96 \times 10^{10}$ ($x = 2.54$ m, $T_w = 60.2^\circ\text{C}$, $T_\infty = 18.0^\circ\text{C}$, measurement only with cold-wire) and $Gr_x = 8.01 \times 10^{10}$ ($x = 2.54$ m, $T_w = 60.3^\circ\text{C}$, $T_\infty = 18.1^\circ\text{C}$, simultaneous measurements using hot- and cold-wires) were compared with those obtained without a promotor (Tsuji and Nagano, 1988a). Fig. 5 shows the dimensionless mean temperature profiles. In the figure, the abscissa denotes the dimensionless coordinate defined by

$$\zeta = (y/x)Nu_{x0}, \quad (1)$$

where Nu_{x0} is the Nusselt number for the turbulent natural convection boundary layer without a promotor as

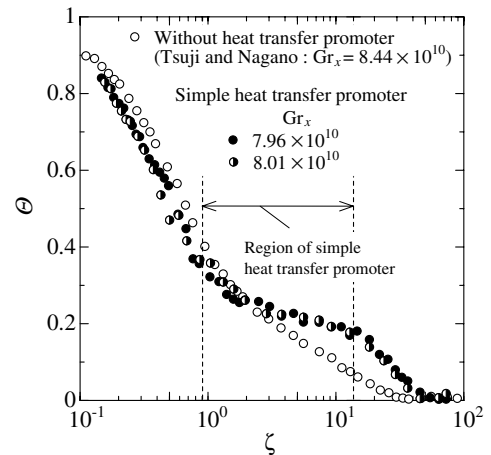


Fig. 5. Mean temperature profiles Θ .

expressed by the following empirical formula (Tsuji and Nagano, 1988a).

$$Nu_{x0} = 0.120(Gr_x Pr)^{1/3} \quad (2)$$

The promoter is placed between the broken lines in Fig. 5. The mean temperature gradient near the wall increases by inserting the promoter, and the mean temperature in the outer region of the boundary layer becomes higher than that without a promoter. This profile of mean temperature is caused because the boundary layer flow slants to the outside of the promoter, and low-temperature fluids in the outer layer invade near the wall with large-scale vortex motions riding out the promoter as mentioned above. The local heat transfer rate estimated from the mean temperature gradient near the wall just coincides with that obtained from electric power supplied to the heated plate.

Mean streamwise velocity profiles measured with normal hot-wires are shown in Fig. 6 in the relation between U/U^* and ζ . Here, U^* is the buoyant velocity ($=\sqrt{g\beta\Delta T_w x}$). Since the flow is blocked out by the promoter and the large-scale vortices approach the wall, mean streamwise velocity becomes somewhat smaller than that without the promoter. Although fluid velocities measured with normal hot-wires include the transverse velocity component, the mean streamwise velocity remains small. However, the mean streamwise velocity increases near the outer edge of the promoter and takes a maximum value in the outer layer. Instantaneous velocity vectors obtained with a PIV in the further downstream region of a simple heat transfer promoter are shown in Fig. 7. It is found that the streamwise velocity near the wall certainly becomes small in that region. As a result, the heat transfer coefficients become worse than those without a promoter. Mean temperature and velocity profiles measured with hot- and cold-wires in the downstream region of the promoter approximately correspond to fluid motions observed in Fig. 4, and it is understood that large-scale vortices induced

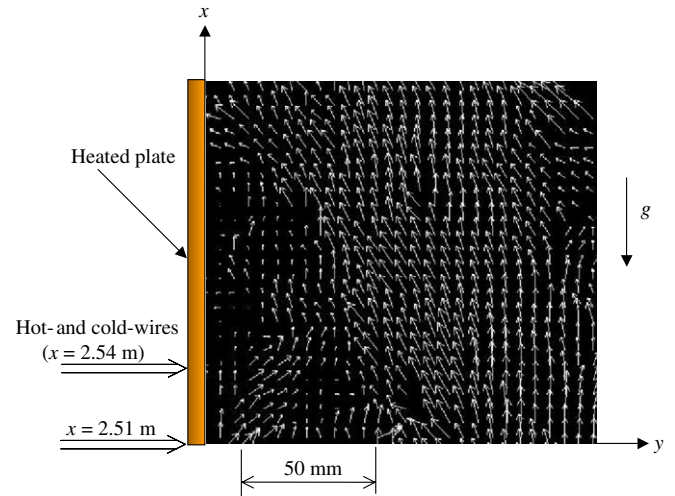


Fig. 7. Instantaneous velocity vectors in the further downstream region of a simple heat transfer promoter.

by the promoter slowly invade near the wall without acceleration behind the promoter.

The distributions of temperature fluctuation intensity $\sqrt{t^2}$ normalized by the temperature difference ΔT_w are shown in Fig. 8. In the case of inserting the simple heat transfer promoter, $\sqrt{t^2}$ slightly increases near the wall and its maximum location approaches the wall as compared to the profile without a promoter. Also, due to the vortex motions riding out the promoter, $\sqrt{t^2}$ near the outer edge of the promoter increases in concert with the mean temperature profile as shown in Fig. 5.

The distributions of streamwise velocity fluctuation intensity $\sqrt{u^2}$ normalized by the buoyant velocity U^* are presented in Fig. 9. The intensity $\sqrt{u^2}$ becomes smaller compared to that without a promoter in the region from the wall to the outer edge of the promoter (note that measured values also include transverse velocity component because of the small streamwise mean velocity). Near the outer edge of the promoter, $\sqrt{u^2}$ takes a maximum value similar to the profile of streamwise mean velocity.

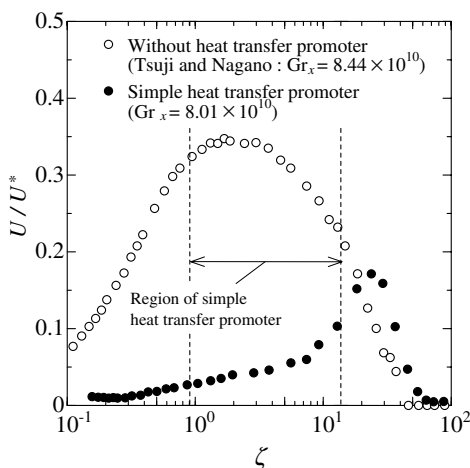


Fig. 6. Mean velocity profiles U/U^* .

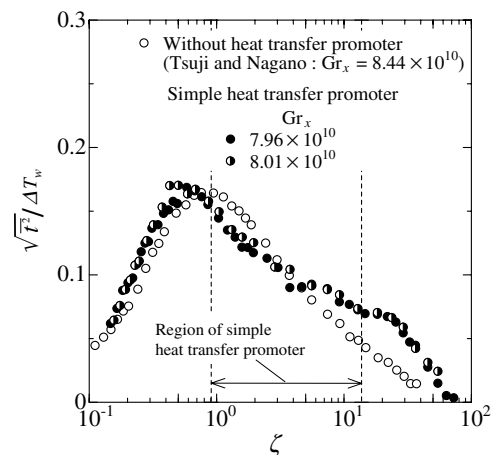


Fig. 8. Intensity of temperature fluctuation $\sqrt{t^2}/\Delta T_w$.

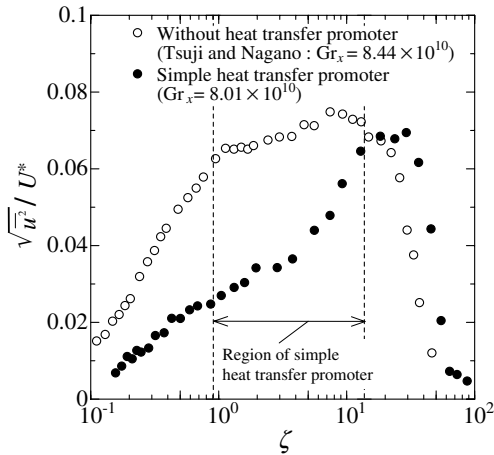


Fig. 9. Intensity of velocity fluctuation $\sqrt{u'}/U^*$.

3.1.4. Heat transfer enhancement with multi-column simple heat transfer promoters

By inserting a simple heat transfer promotor into the boundary layer, the heat transfer coefficient remarkably increases in the region downstream of the promotor, but the heat transfer coefficient decreases in the region further downstream as shown in Fig. 2. To achieve practical heat transfer enhancement, it is required that heat transfer coefficients increase over a wide area of the heated plate. Therefore, we examined whether an increase in heat transfer coefficients could be maintained at a high level by inserting multiple columns of simple heat transfer promoters.

When two simple heat transfer promoters (column number $N=2$) were located at $x=2.33$ m ($x/L=0.58$) and 2.83 m ($x/L=0.71$), where the heat transfer coefficient deteriorates behind the first promotor, with an interval of $I=0.5$ m, and both promoters were set as $(C, \phi, H)=(5$ mm, 45° , 100 mm), the normalized local heat transfer coefficients varied as shown in Fig. 10. Also shown in the figure is the distribution of local heat transfer coefficients obtained by inserting a simple heat transfer promotor located at $x=2.33$ m. The dashed lines indicate the center positions of the two promoters. In the case of employing two simple heat transfer promoters, the heat transfer coefficients increase downstream of each promotor.

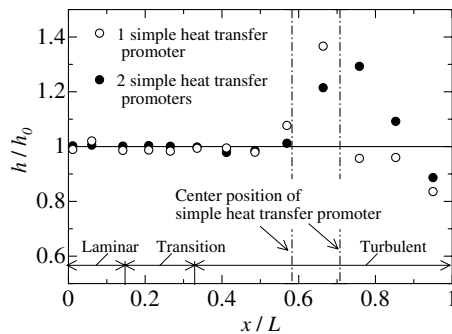


Fig. 10. Distributions of local heat transfer coefficients (simple heat transfer promoters, $N=1$ and 2).

Though the increase rate of heat transfer coefficient is somewhat reduced, the area of heat transfer enhancement broadens compared with the case of a simple heat transfer promotor. In the further downstream of the second promotor, the heat transfer coefficient becomes also worse than that without a promotor.

Next, we examined the variation of heat transfer coefficients for three simple heat transfer promoters. The promoters set as $(C, \phi, H)=(5$ mm, 45° , 100 mm) were located at $x=2.03$, 2.43 and 2.83 m ($x/L=0.51$, 0.61 and 0.71), respectively, with $I=0.4$ m. Fig. 11 shows the variation of normalized heat transfer coefficients from inserting three simple heat transfer promoters. The heat transfer coefficients in the region downstream of the promoters remarkably increase in the wide area of the heated plate compared with those of the two simple heat transfer promoters shown in Fig. 10.

For the insertion of multiple columns of simple heat transfer promoters, the mean rate of heat transfer enhancement associated with the interval I between simple heat transfer promoters and the column number N is presented in Fig. 12 and Table 1. The mean rate of heat transfer enhancement is defined as a ratio of the mean heat transfer coefficients $(h)_m$ in the region from the location $x=\ell$, where the heat transfer coefficient starts to increase by inserting simple heat transfer promoters, to the height $L=4$ m of the heated plate to those without heat transfer promotor $(h_0)_m$ in the same region

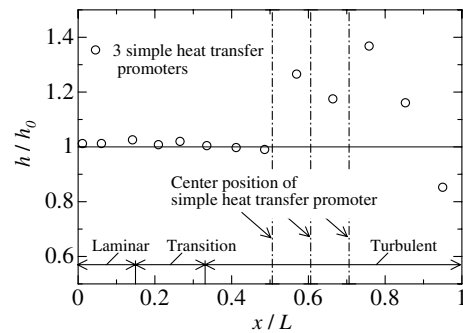


Fig. 11. Distributions of local heat transfer coefficients (simple heat transfer promoters, $N=3$, $I=0.4$ m).

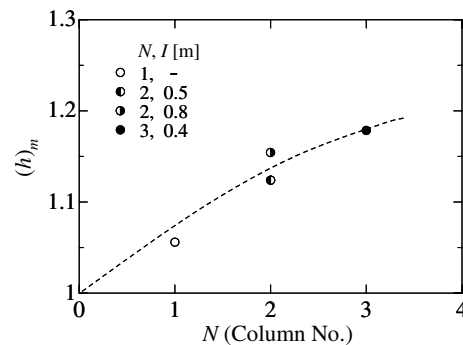


Fig. 12. Mean rate of heat transfer enhancement for simple heat transfer promoters.

Table 1

The mean rates of heat transfer enhancement of the simple heat transfer promoters

N	I [m]	$(h)_m/(h_0)_m$
1	–	1.06
2	0.5	1.12
2	0.8	1.15
3	0.4	1.18

$$(h)_m/(h_0)_m = \int_{\ell}^L h(x)dx / \int_{\ell}^L h_0(x)dx. \quad (3)$$

In the case of the column number $N = 2$, the mean rate of heat transfer rate for $I = 0.8$ m becomes slightly larger than that for $I = 0.5$ m, which indicates that there may be the most appropriate interval between promoters. As the column number N increases, the mean rate of heat transfer enhancement increases by about 18% for the interval $I = 0.4$ m and the column number $N = 3$. Therefore, it becomes clear that heat transfer enhancement in the turbulent natural convection boundary layer can be achieved by inserting simple heat transfer promoters of appropriate columns and intervals in accordance with the height of the heated plate.

3.2. Split heat transfer promoter

The heat transfer coefficients in the turbulent natural convection boundary layer always increase in the region downstream of a simple heat transfer promoter as shown in Fig. 2. However, in the region further downstream, it is also observed that the heat transfer coefficients become worse than those without a promoter due to the deceleration of flow. Therefore, to eliminate the flow stagnancy behind the promoter and strive for more effective heat transfer enhancement, we examined the heat transfer characteristics in the case of short flat plates aligned at fixed intervals in the spanwise direction (split heat transfer promoter) inserted into the natural convection boundary layer.

3.2.1. Heat transfer coefficients for split heat transfer promoter

We located the center positions of three types of split heat transfer promoter aligning 3, 4 and 5 short flat plates ($N_z = 3, 4$ and 5) in the spanwise direction as shown in Fig. 1 at $x = 2.33$ m ($x/L = 0.58$) for the configuration $(C, \phi, H) = (5 \text{ mm}, 45^\circ, 100 \text{ mm})$. The length of short flat plates consisting of the promoter and the clearance between plates in the spanwise direction were made equal tentatively to confirm the efficiency of the promoter. The distributions of local heat transfer coefficients relevant to each promoter varied as presented in Fig. 13. Note that heat transfer rates were obtained from electric power supplied to heaters divided into 13 units in the vertical direction and so it is unable to identify the variation of heat transfer rate in the spanwise direction. The local heat transfer coefficients obtained for a simple heat transfer promoter

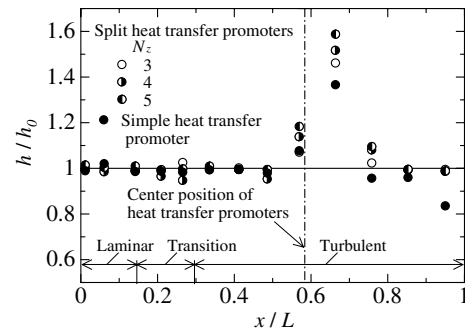


Fig. 13. Distributions of local heat transfer coefficients [split heat transfer promoters (C, ϕ, H) = (5 mm, 45°, 100 mm)].

located at $x = 2.33$ m ($x/L = 0.58$) are also shown in Fig. 13. By inserting split heat transfer promoters into the boundary layer, the local heat transfer coefficients in the region downstream of the promoters increase more than those for the simple heat transfer promoter. For the split heat transfer promoter of $N_z = 5$, the maximum local heat transfer coefficient increases by approximately 60% over that without a promoter. In addition, the deterioration of heat transfer, as observed in the region further downstream of the simple heat transfer promoter, does not occur (for the reason which will be mentioned later). Therefore, it is evident that the split heat transfer promoter consisting of several short flat plates aligned at a fixed interval in the spanwise direction is highly advantageous for heat transfer enhancement compared with the simple heat transfer promoter.

3.2.2. Flow visualization near split heat transfer promoter

For the split heat transfer promoter of $N_z = 5$ located its center position at $x = 2.33$ m, the flow in the x - y plane near the center of the heated plate was visualized with smoke and laser light sheets to clarify the cause of the increase in local heat transfer rates. By locating the split heat transfer promoter of $N_z = 4$ at the same x location, flow visualization in the y - z plane near the heated plate was also conducted (visualized location was $x = 2.54$ m). Examples of captured instantaneous images are shown in Figs. 14 and 15, respectively. In Fig. 14, it is observed that the boundary layer flow detours around the promoter and invades near the wall, forming large-scale vortices similar to those observed with the simple heat transfer promoter as shown in Fig. 4.

However, in Fig. 15, flows heading from the wall to the transverse direction in the clearances between short flat plates slant to the spanwise direction and form longitudinal vortices. Then, low-temperature fluids in the outer region of the boundary layer are conveyed near the wall downstream of the promoter, and high-temperature fluids near the wall are discharged away from the wall in the clearances between the short flat plates. It is conjectured that a series of such fluid behavior contributes largely to the increase in local heat transfer coefficients in the down-

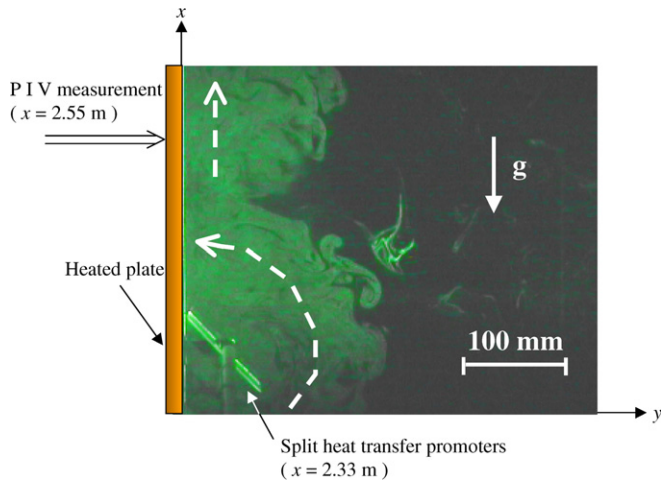


Fig. 14. Visualized fluid motions in the downstream region of a split heat transfer promoter (x - y plane, $N_z = 5$).

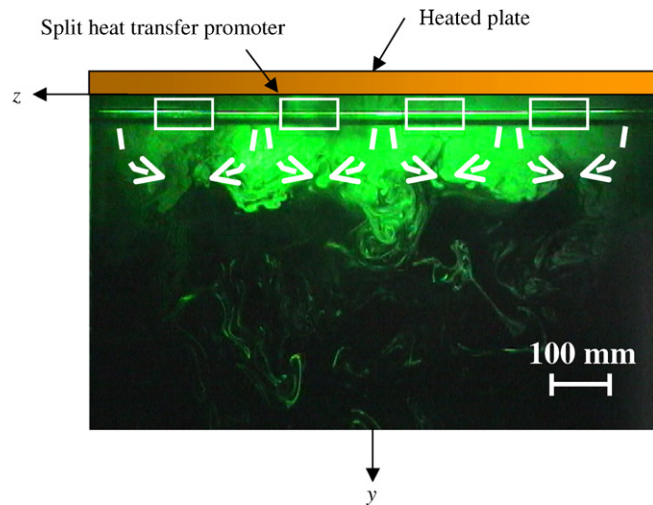


Fig. 15. Visualized fluid motions in the downstream region of a split heat transfer promoter (y - z plane, $N_z = 4$).

stream region of split heat transfer promoters. The fluid behavior as shown in Fig. 15 is never generated with a simple heat transfer promoter, and thus there is no doubt that the longitudinal vortices induced by creating some clearances between short flat plates aligned in the spanwise direction have an important role to play in the heat transfer enhancement of the turbulent natural convection boundary layer.

3.2.3. PIV measurement of flow field for split heat transfer promoter

For the location $x = 2.55$ m (shown with the symbol \Rightarrow in Fig. 14) where the local heat transfer coefficient markedly increased by inserting a split heat transfer promoter, the flow fields in the x - y planes downstream of a short flat plate and clearances between plates were measured with a PIV. Figs. 16–18 show the mean velocities U and V , the intensities of velocity fluctuations $\sqrt{u^2}$ and $\sqrt{v^2}$ and the

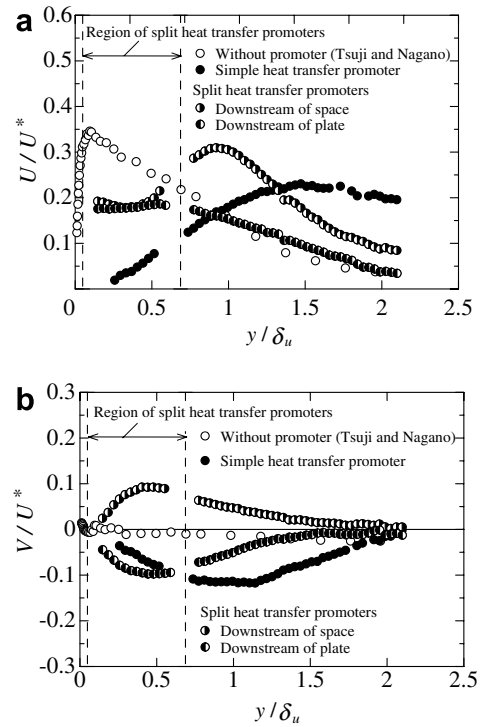


Fig. 16. Mean velocity profiles. (a) Mean streamwise velocity U/U^* (b) Mean transverse velocity V/U^* .

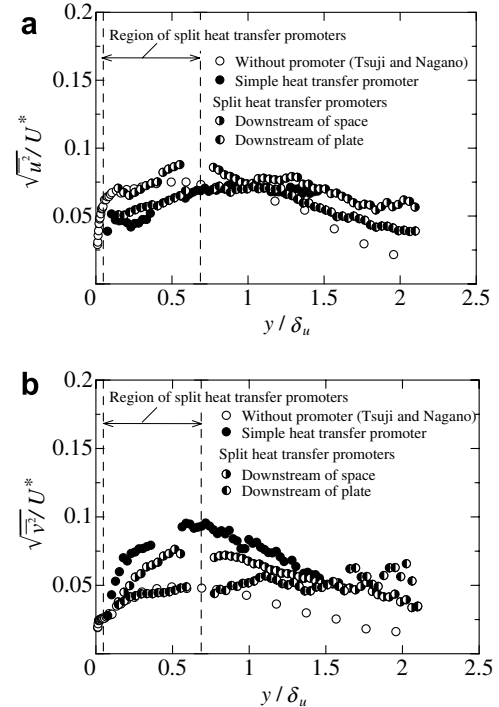


Fig. 17. Intensity of velocity fluctuation. (a) Intensity of velocity fluctuation $\sqrt{u^2}/U^*$ (b) Intensity of velocity fluctuation $\sqrt{v^2}/U^*$.

Reynolds shear stress \overline{uv} normalized by the buoyant velocity U^* , respectively. The measurements for the usual turbulent natural convection boundary layer with hot- and cold-

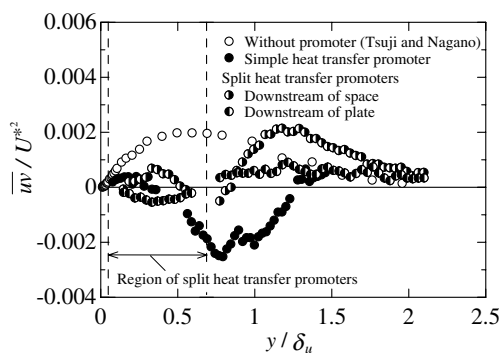


Fig. 18. Reynolds shear stresses.

wires (Tsuji and Nagano, 1988b) and PIV measurements in the region downstream of a simple heat transfer promotor are also presented in the figures. The distance from the wall y is normalized by the integral thickness of the velocity boundary layer δ_u without any promotor (Tsuji and Nagano, 1988b). In these figures, PIV measurements for the region of $y/\delta_u = 0.5$ – 0.6 are excluded because velocity vectors could not be correctly determined under the influence of laser light reflections on acrylic walls installed vertically on either side of the heated plate to keep the two-dimensionality of the boundary layer. The usual turbulent natural convection boundary layer without a promotor was also measured with a PIV, and it was confirmed that the results approximately coincided with the data obtained with hot- and cold-wires in the whole boundary layer region.

As seen in Fig. 16(a), the profile of mean streamwise velocity U in the region downstream of a simple heat transfer promotor becomes very small near the wall and takes a maximum value in the region far beyond the outer edge of the promotor, consistent with the hot-wire data shown in Fig. 6. In contrast, for a split heat transfer promotor, such an extreme decrease in the mean velocity U near the wall does not occur either downstream of the short flat plates or the clearances between plates, though the value of mean velocity becomes somewhat smaller than that without a promotor. It is consequently understood that the clearances between short flat plates aligned in the spanwise direction attenuate the bafflement of flow, and thus split heat transfer promotors do not cause the deterioration of heat transfer in the region further downstream of the promotors as shown in Fig. 13.

The profiles of mean transverse velocity V are presented in Fig. 16(b). In the region downstream of a simple heat transfer promotor, V takes negative values fairly larger than that without a promotor in the whole boundary layer region in association with the movement of large-scale vortices toward the wall. For a split heat transfer promotor, the mean transverse velocity V becomes positive behind the short flat plates and symmetrically negative behind the clearances between the short flat plates similar to the case of a simple heat transfer promotor. These results coincide with flow behavior such that flows heading from the wall to the transverse direction in the clearances between

short flat plates slant to the spanwise direction and form longitudinal vortices approaching the wall downstream of short flat plates as observed in a visualized image shown in Fig. 15. With clearances between plates in the spanwise direction, the streamwise mean velocity U near the wall in the downstream of a split heat transfer promotor is not decelerated inasmuch as a simple heat transfer promotor, and low-temperature fluids invade near the wall in the downstream of short flat plates and high-temperature fluids effectively slip through the clearances between short flat plates. As a result, the local heat transfer coefficients in the region downstream of the split heat transfer promotor increase more than those for the simple heat transfer promotor.

The intensity profiles of streamwise velocity fluctuation $\sqrt{u^2}$ normalized by the buoyant velocity U^* are presented in Fig. 17(a). By inserting a simple heat transfer promotor, $\sqrt{u^2}$ becomes smaller in the region between the wall and the outer edge of the promotor and larger in the region beyond the outer edge of the promotor than that without a promotor. For a split heat transfer promotor, the intensity $\sqrt{u^2}$ downstream of the clearances between short flat plates takes values larger than that without a promotor in the region beyond the outer edge of the promotor. Meanwhile, $\sqrt{u^2}$ behind short flat plates is reduced below that without a promotor in the region between the wall and the outer edge of the promotor and becomes larger than that without a promotor as well as a simple heat transfer promotor.

The intensity profiles of transverse velocity fluctuation intensity $\sqrt{v^2}$ normalized by the buoyant velocity U^* are shown in Fig. 17(b). The intensity $\sqrt{v^2}$ downstream of a simple heat transfer promotor becomes noticeably larger than that without a promotor in the whole boundary layer region. For a split heat transfer promotor, $\sqrt{v^2}$ downstream of the clearances between the short flat plates also becomes larger than that without a promotor over the wide region of the boundary layer and takes a maximum value near the outer edge of the promotor, while $\sqrt{v^2}$ downstream of short flat plates approximately equals that without a promotor in the region between the wall and the outer edge of the promotor and becomes larger than that without a promotor beyond the outer edge of the promotor.

The distributions of Reynolds shear stress \overline{uv} normalized by the buoyant velocity U^* are presented in Fig. 18. In the downstream region of a simple heat transfer promotor, \overline{uv} becomes negative over the wide region of the boundary layer in contrast with that without a promotor and takes a minimum value near the outer edge of the promotor. Therefore, by inserting a simple heat transfer promotor, turbulence production activates in the vicinity of the outer edge of the promotor because of $\partial U/\partial y > 0$ [see Fig. 16(a)] and $\overline{uv} < 0$. For a split heat transfer promotor, \overline{uv} downstream of the clearances between short flat plates takes positive values in the regions of the near-wall and $y/\delta_u > 0.9$ where $\partial U/\partial y < 0$. The Reynolds shear stress \overline{uv} downstream of the short flat plates becomes negative

near the wall and positive in the region beyond the outer edge of the short flat plates where active turbulence production is also caused in association with a positive mean velocity gradient. Such a state may increasingly stimulate turbulent heat transfer.

Instantaneous velocity vectors in the further downstream region of a split heat transfer promoter are presented in Figs. 19 and 20. Fig. 19 shows the velocity vectors behind a short flat plate, it is observed that the boundary layer flow approaches near the wall and the flow stagnancy does not occur. On the other hand, in the downstream of clearances of the plates, the boundary layer flow is directed away from the wall to outer region as shown in Fig. 20. Such fluid motions may be related to the fact that the heat transfer coefficients do not deteriorate in the further downstream region of the split heat transfer promoter.

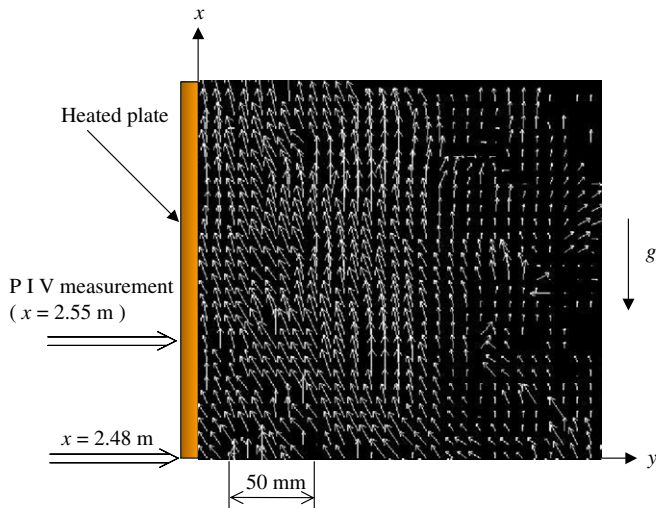


Fig. 19. Instantaneous velocity vectors in the further downstream region of a split heat transfer promoter ($N_z = 5$).

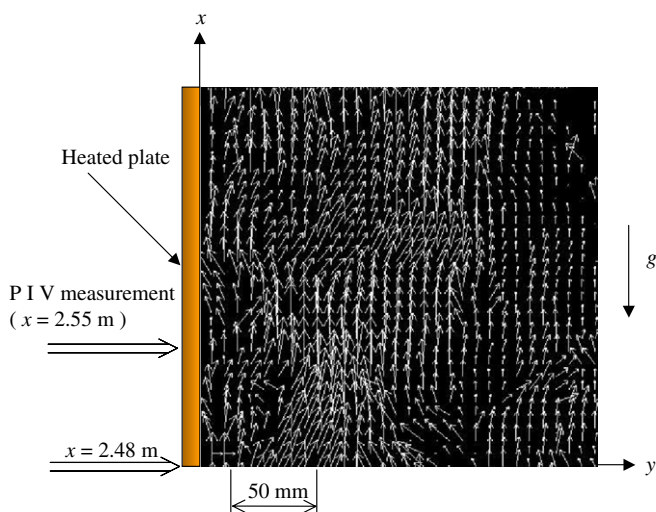


Fig. 20. Instantaneous velocity vectors in the further downstream region of a split heat transfer promoter ($N_z = 4$).

3.2.4. Heat transfer enhancement with multi-column split heat transfer promoters

Although the local heat transfer coefficients for a split heat transfer promoter remarkably increase just behind the promoter above those for a simple heat transfer promoter as shown in Fig. 13, such a favorable state cannot be continued in the farther downstream region of the promoter. Thus, we additionally examined whether high levels of local heat transfer coefficients could be sustained by inserting multi-column split heat transfer promoters near the wall in a vertical direction. The distributions of local heat transfer coefficients obtained for a split heat transfer promoter of $N_z = 5$ locating its center position at $x = 2.33$ m ($x/L = 0.58$) as the first column and a promoter of $N_z = 5$ or $N_z = 4$ locating its center position at $x = 2.83$ m ($x/L = 0.71$) as the second column are presented in Fig. 21. The configuration and size of the short flat plates used conform in all instances to $(C, \phi, H) = (5 \text{ mm}, 45^\circ, 100 \text{ mm})$. Also shown in the figure are local heat transfer coefficients obtained for two simple heat transfer promoters located at the same positions. Concerning multiple split heat transfer promoters, it is found that the area providing high heat transfer coefficients extends in either case of $N_z = 4$ or 5 as the second column, though the heat transfer coefficients downstream of the second column promoter become slightly smaller than those behind the first column promoter.

Moreover, we assessed the mean rate of heat transfer enhancement defined by Eq. (3) for multi-column split heat transfer promoters with the interval $I = 0.5$ m and column number $N = 2$ and compared that with for multi-column simple heat transfer promoters with the same interval and column number. As shown in Table 2, the mean rate of

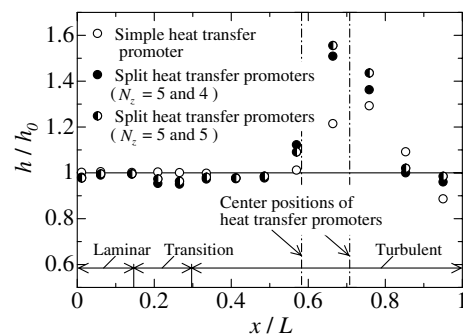


Fig. 21. Distribution of local heat transfer coefficients (split heat transfer promoters, $N = 2$, $I = 0.5$ m).

Table 2

The mean rates of heat transfer enhancement of the split heat transfer promoters

N	N_z	I [m]	$(h)_m/(h_0)_m$
1	3	—	1.11
1	4	—	1.15
1	5	—	1.17
2	5 and 4	0.5	1.20
2	5 and 5	0.5	1.23

heat transfer enhancement obtained for split heat transfer promoters of $N_z = 5$ as the first column and $N_z = 4$ or 5 as the second column is 1.20 or 1.23, respectively. These values substantially exceed the value of 1.12 or 1.15 obtained for multi-column simple heat transfer promoters as shown in Table 1. It should be expected that much higher heat transfer enhancement in excess of approximately 40% for the turbulent natural convection boundary layer can be accomplished by increasing the column numbers of split heat transfer promoters. Thus, the use of split heat transfer promoters is more effective for the heat transfer enhancement in turbulent natural convection compared with simple heat transfer promoters, and the heat transfer coefficients in the wide area of the heated plate can be increased by inserting multi-column split heat transfer promoters.

We consider that more advanced investigations may be required for the optimum shapes of promoters (be not always plates) and the interval of heat transfer promoters in the streamwise direction. Moreover, it is not obvious whether a similar method of heat transfer enhancement is available for different Prandtl number fluids (water, oil, etc.) or not. We also wish to accumulate more useful information on heat transfer enhancement and propose the most suitable promoter, in view of non-dimensional numbers dominating natural convection.

4. Conclusions

The feasibility of heat transfer enhancement was examined by inserting a long flat plate in the spanwise direction (simple heat transfer promoter) and short flat plates aligned at a fixed interval in the spanwise direction (split heat transfer promoter) into the turbulent natural convection boundary layer in air along a vertical heated plate. Results obtained in the present study may be summarized as follows.

1. For a simple heat transfer promoter, the heat transfer coefficient downstream of the promoter exhibits an increase of approximately 37% compared with that observed in the usual turbulent natural convection boundary layer, when the condition of the minimum distance C from the wall to the simple heat transfer promoter, the inclination angle ϕ of the promoter from the vertical direction and the width H of the promoter are 5 mm, 45° and 100 mm, respectively. However, in the region farther downstream region of the promoter, the heat transfer coefficients become lower than those without any promoter.
2. From a flow visualization of the flow field behind a simple heat transfer promoter, it is found that boundary layer flows slant outside of the promoter, and low-temperature fluids in the outer layer invade very near the wall with large-scale vortex motions riding out the promoter and returning to the inner layer. However, high-temperature fluids slipping through the clearances between the wall and promoter get away from the wall and impinge on large vortex motions of low-temperature fluids. Consequently, such fluid motions cause an increase in the local heat transfer coefficient behind the promoter.
3. Heat transfer enhancement in a wide area of the turbulent natural convection boundary layer can be attained by inserting multi-column simple heat transfer promoters at an appropriate interval in accordance with the height of the heated plate.
4. By employing a split heat transfer promoter, the local heat transfer coefficients in the region downstream of the promoter become larger than those for a simple heat transfer promoter and increase approximately 60% compared with those in the usual turbulent natural convection boundary layer. In addition, the deterioration of heat transfer coefficients in the region farther downstream does not occur.
5. From a flow visualization and PIV measurement for a split heat transfer promoter, it was found that the substantial increase of heat transfer coefficients is caused by a joint contribution of longitudinal vortices discharging high-temperature fluids from the clearances between the short flat plates and low-temperature fluid motions climbing the short flat plates.
6. By inserting multi-column split heat transfer promoters in the boundary layer, heat transfer enhancement in all regions of the turbulent natural convection boundary layer could be conducted more effectively compared with inserting multi-column simple heat transfer promoters. It is expected that heat transfer enhancement in excess of approximately 40% for the turbulent natural convection boundary layer could be achieved by placing adequate columns and intervals of the split heat transfer promoters depending on the height of the heated plate.

References

- Han, J.C., Ou, S., Park, J.S., Lei, C.K., 1989. Augmented heat transfer in rectangular channels of narrow aspect ratios with rib turbulators. *Int. J. Heat Mass Transfer* 32, 1619–1630.
- Hattori, Y., Tsuji, T., Nagano, Y., Tanaka, N., 2001. Effects of freestream on turbulent combined-convection boundary layer along a vertical heated plate. *Int. J. Heat Fluid Flow* 22, 315–322.
- Hu, Z., Shen, J., 1996. Heat transfer enhancement in a converging passage with discrete ribs. *Int. J. Heat Mass Transfer* 39, 1719–1727.
- Komori, K., Inagaki, T., Kito, S., Mizoguchi, N., 1999. Natural convection heat transfer along a vertical flat plate with a projection in the turbulent region. *JSME B* 65, 4049–4054, in Japanese.
- Lau, S.C., Kukreja, R.T., McMillin, R.D., 1991. Effects of V-shaped rib arrays on turbulent heat transfer and friction of fully developed flow in a square channel. *Int. J. Heat Mass Transfer* 34, 1605–1616.
- Meinders, E.R., Van der Meer, T.H., Hanjalić, K., 1998. Local convective heat transfer from an array of wall-mounted cubes. *Int. J. Heat Mass Transfer* 41, 335–346.
- Misumi, T., Kitamura, K., 1999. Enhancement of natural convective heat transfer from tall, vertical heated plates. *JSME B* 65, 4041–4048, in Japanese.

- Savill, A.M., Mumford, J.C., 1988. Manipulation of turbulent boundary layers by outer-layer devices: skin-friction and flow-visualization results. *J. Fluid Mech.* 191, 389–418.
- Sturgis, J.C., Mudawar, I., 1999. Single-phase heat transfer enhancement in a curved, rectangular channel subjected to concave heating. *Int. J. Heat Mass Transfer* 42, 1255–1272.
- Tsuji, T., Nagano, Y., 1988a. Characteristics of a turbulent natural convection boundary layer along a vertical flat plate. *Int. J. Heat Mass Transfer* 31, 1723–1734.
- Tsuji, T., Nagano, Y., 1988b. Turbulence measurements in a natural convection boundary layer along a vertical flat plate. *Int. J. Heat Mass Transfer* 31, 2101–2111.
- Tsuji, T., Nagano, Y., 1989. Velocity and temperature measurements in a natural convection boundary layer along a vertical flat plate. *Exp. Thermal Fluid Sci.* 2, 208–215.
- Tsuji, T., Nagano, Y., Tagawa, M., 1992. Experiment on spatio-temporal turbulent structures of a natural convection boundary layer. *ASME J. Heat Transfer* 114, 901–908.